HHS Public Access

Author manuscript

Neuropeptides. Author manuscript; available in PMC 2017 August 01.

Published in final edited form as:

Neuropeptides. 2017 August ; 64: 75–83. doi:10.1016/j.npep.2016.12.005.

Embryonic ablation of neuronal VGF increases energy expenditure and reduces body weight

Cheng Jiang[1,5,#], **Wei-Jye Lin**[1,#], **Masato Sadahiro**[1,5], **Andrew C. Shin**[2], **Christoph Buettner**[1,2], and **Stephen R. Salton**[1,3,4,*]

[1]Department of Neuroscience, Icahn School of Medicine at Mount Sinai, New York, NY, 10029-6574, USA

[2] Department of Medicine, Icahn School of Medicine at Mount Sinai, New York, NY, 10029-6574, USA

[3]Department of Geriatrics, Icahn School of Medicine at Mount Sinai, New York, NY, 10029-6574, USA

[4]Friedman Brain Institute, Icahn School of Medicine at Mount Sinai, New York, NY, 10029-6574, USA

[5]Graduate School of Biomedical Sciences, Icahn School of Medicine at Mount Sinai, New York, NY, 10029-6574, USA

Abstract

Germline ablation of VGF, a secreted neuronal, neuroendocrine, and endocrine peptide precursor, results in lean, hypermetabolic, and infertile adult mice that are resistant to diet-, lesion-, and genetically-induced obesity and diabetes (Hahm et al., 1999, 2002). To assess whether this phenotype is predominantly driven by reduced VGF expression in developing and/or adult neurons, or in peripheral endocrine and neuroendocrine tissues, we generated and analyzed conditional VGF knockout mice, obtained by mating loxP-flanked (floxed) *Vgf* mice with either pan-neuronal Synapsin-Cre- or forebrain alpha-CaMKII-Cre-recombinase-expressing transgenic mice. Adult male and female mice, with conditional ablation of the *Vgf* gene in embryonic neurons had significantly reduced body weight, increased energy expenditure, and were resistant to diet-induced obesity. Conditional forebrain postnatal ablation of VGF in male mice, primarily in adult excitatory neurons, had no measurable effect on body weight nor on energy expenditure, but led to a modest increase in adiposity, partially overlapping the effect of AAV-Cre-mediated targeted ablation of VGF in the adult ventromedial hypothalamus and arcuate nucleus of floxed

[*]Corresponding author: Dr. Stephen R. J. Salton, Department of Neuroscience, Box 1639, Icahn School of Medicine at Mount Sinai, One Gustave L. Levy Place, New York NY, 10029 USA, Tel: 212-824-9308; Fax: 646-537-9583, stephen.salton@mssm.edu.
[#]Equal contribution

Disclosure Statement: The authors have nothing to disclose.

Contributions

SS, CB, WJL, ACS, and CJ designed the study. MS and SS generated the targeting constructs and floxed VGF line; CJ, MS, and WJL generated the $Vgf^{flpflox}$ line, genetic crosses with *Syn-Cre* and α*CaMKII-Cre* transgenic lines, and genotyped mice for metabolic analysis; CJ, WJL, and ACS carried out metabolic phenotyping and analyzed data; WJL carried out immunohistochemistry and western analysis; CJ and SS wrote the manuscript with the input of co-authors; all authors approved the final version of the manuscript.

Vgf mice (Foglesong et al., 2016), and also consistent with results of icv delivery of the VGF-derived peptide TLQP-21 to adult mice, which resulted in increased energy expenditure and reduced adiposity (Bartolomucci et al., 2006). Because the lean, hypermetabolic phenotype of germline VGF knockout mice is to a great extent recapitulated in *Syn-Cre*$^{+/-}$, *Vgf*$^{flpflox/flpflox}$ mice, we conclude that the metabolic profile of germline VGF knockout mice is largely the result of VGF ablation in embryonic CNS neurons, rather than peripheral endocrine and/or neuroendocrine cells, and that in forebrain structures such as hypothalamus, VGF and/or VGF-derived peptides play uniquely different roles in the developing and adult nervous system.

Keywords

adipose; brain-derived neurotrophic factor (BDNF); chromogranin; diet-induced obesity; energy expenditure; hypothalamus; neuropeptide; secretogranin; Synapsin-Cre; VGF (non-acronymic)

1. INTRODUCTION

VGF is a secreted granin-like protein and peptide precursor that is expressed in CNS and PNS neurons and in several neuroendocrine and endocrine tissues (Bartolomucci et al., 2011; Levi et al., 2004; Salton et al., 2000), and in hypothalamus, expression is regulated by nutritional status (Hahm et al., 2002; Hahm et al., 1999; Saderi et al., 2014; Toshinai et al., 2010). Homozygous germline VGF knockout mice are lean and hypermetabolic, and resist developing obesity and diabetes when fed a high fat diet (Hahm et al., 1999). Targeted deletion of *Vgf* also suppresses obesity, hyperinsulinemia and hyperglycemia in *A*^{y}*/a* agouti and melanocortin 4 receptor knockout mice (Hahm et al., 2002; Watson et al., 2005), supporting a role for VGF in the melanocortin pathway. VGF signals, at least in part, through the binding of the VGF-derived peptide TLQP-21 to two recently identified receptors, the G-protein coupled C3a complement receptor (Cero et al., 2014; Hannedouche et al., 2013) and/or the gC1q complement receptor (Chen et al., 2013). Recent studies demonstrate that C3aR1 is likely to be the critical TLQP-21 receptor for central and peripheral metabolic regulation, working in concert with beta-adrenergic receptors to regulate lipolysis, body weight and adiposity (Cero et al., 2016). Data further indicate that VGF and the VGF-derived peptide TLQP-21 regulate energy balance by modulating sympathetic outflow to peripheral metabolic tissues (Bartolomucci et al., 2006; Possenti et al., 2012; Watson et al., 2009) through mechanisms that may be mediated by VGF-derived peptides or by the ‘granulogenic’ function of VGF in large dense core vesicles (LDCVs) and the secretory pathway (Fargali et al., 2014). In addition to VGF C-terminal peptides, the NERP peptides, including NERP-1 and NERP-2, which are selectively expressed in neuroendocrine, endocrine and neural tissues (Mishiro-Sato et al., 2010; Noli et al., 2015; Yamaguchi et al., 2007), have been demonstrated to regulate energy expenditure, feeding behavior via the orexin system, and/or insulin secretion, via effects on hypothalamic neurosecretory cells and pancreatic beta cells (Kim et al., 2015; Melis et al., 2012; Moin et al., 2012; Toshinai et al., 2010; Yamaguchi et al., 2007).

In agreement with the demonstration that TLQP-21 administration increases energy expenditure and lipolysis (Bartolomucci et al., 2006; Possenti et al., 2012), recent AAV-Cre-

mediated ablation of VGF in the adult hypothalamus, targeting arcuate nucleus (Arc) and ventromedial hypothalamus (VMH), of loxP-flanked (floxed) VGF mice ($Vgf^{flpflox/flpflox}$), reduced energy expenditure and increased adiposity in males (Foglesong et al., 2016).

Despite these advances, the precise roles that neuronal and endocrine VGF play in developing and adult animals are incompletely understood. Here we utilize $Vgf^{flpflox/flpflox}$ mice, with the $VGF_{1–617}$ coding sequence flanked by loxP recombination sites and the FRT-flanked neomycin selection cassette removed (Lin et al., 2015; Sadahiro et al., 2015), to determine whether conditional *Vgf* gene ablation in embryonic neurons is the predominant driver of increased energy expenditure and reduced body weight in adult germline homozygous VGF knockout mice. To carry out these experiments, we used transgenic Syn1-Cre mice, which express Cre-recombinase in most neurons from embryonic day E12.5, including in the cortex, hippocampus, cerebellum and spinal cord (Zhu et al., 2001), leading to the ablation of floxed genes throughout the brain, and in spinal cord, dorsal root ganglia, and testis, but not in a number of non-neural tissues (Cohen et al., 2001; Hasue et al., 2005; Mori et al., 2004; Rempe et al., 2006; Ren et al., 2013; Zhu et al., 2001), and αCaMKII-Cre transgenic mice, with expression largely restricted to adult forebrain hippocampal excitatory pyramidal CA1 neurons (Tsien et al., 1996).

2. MATERIALS AND METHODS

2.1. Mouse Strains and Diets

The floxed VGF mouse line was generated as recently described (Lin et al., 2015) by inserting a 5’ flanking loxP site into the *Vgf* 5’ UTR (KpnI site), and a 3’ flanking loxp site and FRT-flanked neomycin selection cassette, derived from p-loxP-2FRT-PGKneo (Dr. David Gordon, University of Colorado Health Science Center), into the *Vgf* 3’ UTR (XbaI site), using previously described mouse *Vgf* genomic sequences (Hahm et al., 1999). Mice with germline transmission of the targeted, floxed *Vgf* allele (Vgf^{flox}) were then crossed with FLPe-recombinase expressing mice driven by the *Gt(ROSA)26Sor* promoter (JAX: 009086; The Jackson Laboratory; C57BL/6J background). Mice lacking the FRT-flanked PGK-neo cassette in the germline ($Vgf^{flp/flox}$) were backcrossed for two additional generations to C57BL/6J, and experiments were performed on $Vgf^{flp/flox}$ mice with a background that is >98% C57BL/6J (MaxBac, Charles River). The entire coding sequence of $VGF_{1–617}$ and all identified VGF-derived peptides are therefore flanked by loxp sites and are removed by conditional gene ablation.

To generate a conditional neuronal knock-out of VGF ($Syn\text{-}Cre, Vgf^{flpflox/flpflox}$), we bred male mice that carried the conditional VGF knock-out allele with female mice that carried the synapsin I promoter-driven Cre recombinase allele (JAX: 003966; The Jackson Laboratory; C57BL/6 background) (Zhu et al., 2001), to prevent possible germline VGF ablation (Rempe et al., 2006). A similar breeding scheme was used to generate forebrain knockout of VGF in $\alpha CaMKII\text{-}Cre, Vgf^{flpflox/flpflox}$ mice (JAX: 005359; T29-1Stl; The Jackson Laboratory; C57BL/6 background) (Tsien et al., 1996). $Syn\text{-}Cre, Vgf^{flpflox/flpflox}$ mice were analyzed at 9–20 weeks of age (standard diet) or 14–21 weeks of age (high fat diet), and $\alpha CaMKII\text{-}Cre, Vgf^{flpflox/flpflox}$ mice were analyzed at 16–18 weeks of age (standard diet).

Mice were housed at room temperature in a 12h light, 12h dark cycle, with chow and water available ad lib unless otherwise specified. Mice fed control chow (STD) received a 10% fat, 70% carbohydrate, 20% protein, 3.85 kcal/g diet, and mice fed high fat chow (HFD) received a 60% fat, 20% carbohydrate, 20% protein, 5.24 kcal/g diet (Research Diets; New Brunswick, NJ). Mice were weaned at 21 days of age onto STD, and subgroups were fed HFD or STD for 6–10 weeks starting at 8–11 weeks of age; daily food consumption was measured over 4 consecutive days during the 6^{th} or 10^{th} week of STD/HFD. Mice were group-housed in a standard, non-enriched environment, unless individually housed for metabolic monitoring. All animal studies were conducted in accordance with the Guide for Care and Use of Experimental Animals, using protocols approved by Institutional Animal Care and Use Committees at the Icahn School of Medicine at Mount Sinai.

2.2. Metabolic Cage and Body Composition Analyses

Metabolic monitoring systems were used to evaluate activity, food consumption, and energy expenditure, including comprehensive animal metabolic monitoring systems (PhenoMaster/LabMaster, TSE Systems, Chesterfield, MO). Mice were individually housed for metabolic testing, and were habituated to the metabolic chamber for 1 day prior to collection of data for up to 6 additional days (cohort sizes for each sex, genotype, and diet are listed in the figures and/or figure legends). VO_2, energy expenditure, and respiratory exchange ratio (RER) were calculated from the gas-exchange data. Activity was measured on the×axis with the use of infrared beams. Live and carcass cohorts were analyzed for total body fat, lean tissue, and body water content using an EchoMRI quantitative magnetic resonance system (Echo Medical Systems, Houston, TX).

2.3. Immunohistochemical Analysis

Mice were anesthetized with ketamine/xylazine and intracardially perfused with ice cold 4% paraformaldehyde in PBS. Brains were post-fixed for 4 hr at 4°C before Leica VT 1000S vibratome sectioning (50 μm), and free-floating sections were permeabilized with 0.2% Triton X-100 in PBS at 25°C, then blocked in 3% goat serum and 5% bovine serum albumin (BSA) with 0.05% Triton X-100 in PBS for 1hr. Sections were incubated overnight at 4°C in the following antibody dilutions: anti-VGF C-terminal (rabbit polyclonal anti-AQEE-30) (Chakraborty et al., 2006) (1:2000) in 5% BSA. Sections were washed the next day with 0.2% Triton X-100 in PBS, incubated in 1:500 goat anti-rabbit Texas Red X (Life Technologies, Grand Island, New York) in PBS for 1 hr, and then were washed again. Sections were stained with DAPI, mounted with antifade solution (Life Technologies), and imaged by Zeiss LSM780 confocal microscopy.

2.4. Statistics

Values are presented as the mean ± SEM. Comparisons among groups were made by ANOVA and Tukey's or Bonferroni post-hoc testing, using GraphPad Prism v5.0. Differences were considered statistically significant at $p < 0.05$. 3.

RESULTS

3.1. Immunohistochemical analysis reveals that VGF expression is robustly reduced in hypothalamus and hippocampus in adult *Syn-Cre,Vgf*$^{flpflox/flpflox}$ mice, while VGF expression in these regions is more modestly reduced in adult αCaMKII-*Cre,Vgf*$^{flpflox/flpflox}$ mice

To determine whether VGF expression in adult Syn-Cre conditional knockout mice was regionally reduced as anticipated based on the previously reported pan-neuronal (Cohen et al., 2001; Hasue et al., 2005; Mori et al., 2004; Rempe et al., 2006; Ren et al., 2013; Zhu et al., 2001) expression of Cre-recombinase in this transgenic line, we perfused and immunostained 4-month old *Syn-Cre,Vgf*$^{flpflox/flpflox}$ male mice (Fig. 1B, D, F, H and J), and age- and sex-matched *Vgf*$^{flpflox/flpflox}$ wild type controls (Fig. 1A, C, E, G and I). Syn-Cre expression resulted in widespread downregulation of VGF expression throughout the adult brain, shown here in hypothalamus, including suprachiasmatic nucleus (SCN; Fig. 1A–B), paraventricular hypothalamus (PVH; Fig. 1C–D), and arcuate (ARC; Fig. 1E–F), hippocampus (HC; Fig. 1G–H), and cerebral cortex (CC; somatosensory cortex layers 1 and 2/3; Fig. 1I–J). For comparison, VGF protein levels in adult adrenal gland isolated from *Syn-Cre,Vgf*$^{flpflox/flpflox}$ and *Vgf*$^{flpflox/flpflox}$ wild type mice were comparable (Supp. Fig. 1).

We further examined expression of VGF in forebrain conditional knockout mice driven by transgenic αCaMKII-Cre (Tsien et al., 1996). In adult 5–7 month old α*CaMKII-Cre,Vgf*$^{flpflox/flpflox}$ mice (Supp. Fig. 2A–F), α*CaMKII-Cre* expression led to a more modest reduction of VGF in hypothalamus (PVH) and hippocampus [reducing VGF primarily in excitatory neurons, sparing interneurons, as previously shown (Lin et al., 2015)] (Supp. Fig. 2A–F).

3.2. Adult male and female mice with $VGF_{1–617}$ ablated in embryonic neurons have reduced body weight and increased energy expenditure, and are resistant to diet-induced obesity, compared to wild type controls

To determine whether ablation of neuronal VGF was the major driver of the lean, hypermetabolic phenotype that has been previously described in germline VGF knockout mice, we generated conditional knockout mice utilizing *Vgf*^{flpflox} mice (Lin et al., 2015), which have the entire VGF coding sequence on a single exon flanked by loxP recombination sites, and mated these with the Synapsin-Cre transgenic line, which expresses Cre-recombinase in all CNS neurons and a subset of dorsal root ganglia (DRG) sensory neurons, starting approximately at embryonic day E12 (Zhu et al., 2001). Male mice lacking neuronal VGF and wild type controls were analyzed at 9–20 weeks of age. As shown in Fig. 2 (panels A and D), male *Syn-Cre,Vgf*$^{flpflox/flpflox}$ mice had reduced body weight and increased energy expenditure, compared to either wild type (+/+,+/+), (*Syn-Cre,+/+*), or (*+/+,Vgf*$^{flpflox/flpflox}$) controls, and thus male mice with targeted knockout in E12 neurons of the floxed *Vgf* alleles showed a similar phenotype to that described for germline VGF knockout mice (Hahm et al., 2002; Hahm et al., 1999). Body composition (% normalized to body weight) in conditional knockout mice was similar to controls, suggesting proportional decreases in both fat and lean mass (Fig. 2B–C). Food intake (Fig. 2F) was not reduced in male *Syn-Cre,Vgf*$^{flpflox/flpflox}$ mice, unlike homozygous germline VGF knockout mice in

which it is increased (Hahm et al., 2002; Hahm et al., 1999), and locomotor activity and RER did not significantly differ from wild type males (Fig. 2E and 2G). Parallel studies in 9–20 week old female *Syn-Cre,Vgf*$^{flpflox/flpflox}$ mice revealed reduced body weight (Fig. 3A), no change in fat or lean mass normalized to body weight (Fig. 3B–C), and increased energy expenditure (Fig. 3D), without a difference in food intake, RER, or locomotor activity (Fig. 3E–G) compared to wild type females.

Because germline VGF knockout mice resist diet-, genetic-, and lesion-induced obesity (Hahm et al., 2002; Hahm et al., 1999), we tested adult male (Fig. 4) and female (Fig. 5) *Syn-Cre,Vgf*$^{flpflox/flpflox}$ mice, with embryonic pan-neuronal ablation of VGF, to determine whether they were resistant to diet-induced obesity (DIO). Mice were weaned at 21 days onto standard chow diet (STD), and were fed either STD or a high-fat diet (HFD) for 6–10 weeks starting at 8–11 weeks of age. Body weights of male (Fig. 4A) and female (Fig. 5A) *Syn-Cre,Vgf*$^{flpflox/flpflox}$ mice fed HFD were measured weekly over 6 weeks, and conditional knockout mice were found to be significantly resistant to diet-induced obesity compared to wild type mice. After 6–10 weeks of HFD compared to STD, body weights, body composition and metabolic parameters were measured. Body weights of 4–5 month old male and female *Syn-Cre,Vgf*$^{flpflox/flpflox}$ mice on HFD for 6 weeks and those of sex- and age-matched *Syn-Cre,Vgf*$^{flpflox/flpflox}$ mice on STD were not significantly different (Figs. 4B and 5B). Male wild type mice (+/+,+/+; *Syn-Cre,+/+*; or *+/+,Vgf*$^{flpflox/flpflox}$) fed HFD had significantly increased body weights compared to mice of the same genotype fed STD (Fig. 4B); in females, wild type *+/+,Vgf*$^{flpflox/flpflox}$ mice had significantly higher body weights on HFD compared to STD, while *Syn-Cre,+/+* mice did not, perhaps due to the small size of this age-matched cohort (n=2) (Fig. 5B). In addition, body weights of *Syn-Cre,Vgf*$^{flpflox/flpflox}$ mice fed HFD for 6–10 weeks were significantly reduced compared to HFD-fed, sex- and age-matched wild type mice (Figs. 4C and 5C), as was fat mass (Figs. 4D and 5D), while lean mass was significantly increased (Figs. 4E and 5E). Energy expenditure of *Syn-Cre,Vgf*$^{flpflox/flpflox}$ male and female mice on a HFD was also robustly increased compared to HFD-fed, sex- and age-matched wild type mice (Figs. 4F and 5F). Lastly, food intake for male *Syn-Cre,Vgf*$^{flpflox/flpflox}$ mice was reduced for two dark cycles compared to +/+, *Vgf*$^{flpflox/flpflox}$, while locomotor activity was consistently increased, and RER remained unchanged, compared to wild type male mice; RER, food consumption, and locomotor activities in female *Syn-Cre,Vgf*$^{flpflox/flpflox}$ and wild type mice fed HFD were not significantly different (Figs. 4G–I and 5G–I).

3.3. Adult mice with ablation of VGF$_{1–617}$ in postnatal forebrain excitatory neurons have similar body weight, lean body mass, and energy expenditure, but increased fat mass, compared to wild type controls

As male and female *Syn-Cre,Vgf*$^{flpflox/flpflox}$ mice with pan-neuronal ablation of VGF early in development largely phenocopied homozygous germline VGF knockout mice, we examined whether more targeted neuronal *Vgf* gene excision, in adult forebrain excitatory neurons of α*CaMKII-Cre,Vgf*$^{flpflox/flpflox}$ mice, reduced body weight and increased energy expenditure. In contrast to germline or embryonic pan-neuronal *Vgf* gene ablation, we noted no change in body weight, lean body mass, energy expenditure, locomotor activity, or food intake, but observed a modest, significant increase in fat mass (% adipose relative to body

weight) in male 16-week old αCaMKII-Cre,$Vgf^{flpflox/flpflox}$ mice fed a regular chow diet compared to wild type mice (Supp. Fig. 3).

4. DISCUSSION

Our experiments suggest that the robust effect of germline *Vgf* gene knockout to reduce body weight and fat mass, and increase energy expenditure (Fargali et al., 2012; Hahm et al., 2002; Hahm et al., 1999; Watson et al., 2009; Watson et al., 2005), are primarily the result of VGF ablation in embryonic neurons. The synapsin-1 promoter in transgenic Syn1-Cre mice (Jackson Laboratory #003966) drives Cre-recombinase expression that is detectable at embryonic day E12.5 in most neurons, including in the cortex, hippocampus, cerebellum and spinal cord (Zhu et al., 2001), and leads to the ablation of floxed genes in the brain, including in cerebrum, hippocampus, hypothalamus, and brain stem, and in spinal cord, dorsal root ganglia, and testis, but not in pancreas, heart, liver, skeletal muscle, white and brown adipose, lung, ovary, spleen, and kidney (Cohen et al., 2001; Hasue et al., 2005; Mori et al., 2004; Rempe et al., 2006; Ren et al., 2013; Zhu et al., 2001); within the CNS, regional variation in recombination has been noted (Cohen et al., 2001; Ren et al., 2013; Zhu et al., 2001), with almost complete loss in most cortical neurons, particularly large pyramidal neurons (May et al., 2004), but not in glial cells or neural progenitors (Zhu et al., 2001). Syn-Cre transgenic mice were chosen over the Nestin-Cre line, which also drives ablation of floxed genes in CNS neurons, because mice carrying this latter transgene have a marked metabolic phenotype (Briancon et al., 2010; Galichet et al., 2010; Harno et al., 2013), while in our studies (Figs. 2–5), Syn-Cre mice were metabolically indistinguishable from (+/+,+/+) or (+/+, $Vgf^{flpflox/flpflox}$) wild type controls.

Conditional *Vgf* gene ablation in *Syn-cre,* $Vgf^{flpflox/flpflox}$ mice, in most embryonic CNS neurons, increased energy expenditure and decreased body weight in adult males and females fed either STD or HFD, while on a HFD, *Syn-cre,* $Vgf^{flpflox/flpflox}$ had reduced fat and increased lean mass, and in males only, increased locomotor activity and reduced food consumption, compared to wild type mice, to a large extent phenocopying the robust effect of global, germline *Vgf* gene ablation (Fargali et al., 2012; Hahm et al., 2002; Hahm et al., 1999; Watson et al., 2009; Watson et al., 2005). Underlying mechanisms or circuits that may explain these small differences between male and female conditional VGF knockout mice are currently unknown. Preliminarily, with relatively fewer mice analyzed, forebrain *Vgf* gene ablation in $Vgf^{flpflox/flpflox}$,α*CaMKII-cre* mice, in adult excitatory neurons, resulted in a small increase in adiposity but did not affect body weight, feeding, and energy expenditure (Supp. Figs. 2–3). Taken together, these data are consistent with the following conclusions: (1) the lean, hypermetabolic phenotypes of adult $Vgf^{-/-}$ knockout mice (Hahm et al., 2002; Hahm et al., 1999) and adult $Vgf^{+/-}$ heterozygote knockout mice (Sadahiro et al., 2015) are a likely consequence of an important functional role of VGF in developing neural circuits that regulate energy balance, (2) the hypermetabolic phenotype and associated resistance to obesity and diabetes result from a loss of neuronal VGF during development, (3) lack of endocrine and/or neuroendocrine VGF in germline knockout mice is unlikely to play a critical role in the development of this lean phenotype, and (4) preliminary analysis of mice that have *Vgf* ablated in adult forebrain excitatory neurons, resulting in a modest increase in fat mass, reveal a phenotype opposite to mice treated with intracerebroventricular (icv)

VGF-derived peptide TLQP-21, consistent with a critical role for TLQP-21 in the adult to regulate energy balance. Indeed, chronic icv administration of the VGF-derived peptide TLQP-21 increased energy expenditure and body temperature and limited diet-induced obesity in mice (Bartolomucci et al., 2006), and decreased food intake, body weight and adiposity in Siberian hamsters (Jethwa et al., 2007). Peripheral ip administration of TLQP-21 increased lipolysis (Possenti et al., 2012), and enhanced glucose-stimulated insulin secretion in human and rat islets and improved glycemic control *in vivo* (Stephens et al., 2012), but had no effect on hormone secretion in perfused rat pancreas (Christiansen et al., 2015).

As seen in previous studies of heterozygous germline VGF knockout mice (Sadahiro et al., 2015), we noted not only decreased fat mass in Syn-Cre conditional VGF knockout mice, but also increased lean mass in males and females fed a HFD (Figs. 4–5, panel E). The underlying mechanism(s) by which reduced neuronal VGF expression results in increased lean mass are currently unknown. However, much of lean mass is likely skeletal muscle, which along with brown adipose tissue (BAT) is an important site of non-shivering thermogenesis (Silva, 2011), and makes the major contribution to energy expenditure during rest and exercise (Butler and Kozak, 2010). Additional studies would be required to investigate whether changes in skeletal muscle gene expression in Syn-Cre conditional VGF knockout mice drive increased mitochondrial function and skeletal muscle thermogenesis. Activity and non-activity related energy expenditure contribute to total energy expenditure (Virtue et al., 2012). We did not observe increased locomotor activity in male or female Syn-Cre conditional knockout mice fed STD, but on a HFD, noted increased dark-phase locomotor activity in males. Thus it remains possible in male Syn-Cre conditional VGF knockout mice, that at least a component of the increased energy expenditure noted in HFD-fed males could result from activity, which we found previously to increase in mice that express truncated $VGF_{1–524}$ knocked into the *Vgf* locus, and therefore lack several C-terminal peptides including TLQP-21 (Sadahiro et al., 2015).

Targeted hypothalamic knockdown of VGF in the adult ARC/VMH resulted in decreased energy expenditure and body temperature, decreased locomotor activity, and increased adiposity, but did not change body weight or food intake, in AAV-Cre:GFP injected male $Vgf^{flpflox/flpflox}$ mice (Foglesong et al., 2016), similar to the preliminary analysis of $\alpha CaMKII\text{-}cre, Vgf^{flpflox/flpflox}$ presented here. Our data are therefore consistent with significantly different VGF functions in the developing and adult forebrain, particularly hypothalamus, to regulate energy and glucose balance. By contrast, targeted AAV-Cre-mediated VGF knockdown in adult hippocampus and global germline VGF ablation result in very similar effects on contextual fear memory and depressive behavior [(Lin et al., 2015) and unpublished data], suggesting different developmental roles for VGF in hypothalamic and hippocampal forebrain circuits, and potentially the function of distinct bioactive VGF peptides in the hypothalamus during development and in the adult. Moreover, these data are also consistent with a metabolic role for VGF in the adult hypothalamus that is downstream of BDNF/TrkB signaling. Intracerebroventricular (icv) infusion or targeted hypothalamic administration of BDNF generally increases energy expenditure, reduces feeding, and reduces body weight, while conditional CNS or hypothalamic *Bdnf* gene ablation generally leads to obesity (Noble et al., 2011), for the most part paralleling effects of icv TLQP-21

peptide administration and conditional hypothalamic *Vgf* gene ablation in the adult, respectively. Activating the hypothalamic-sympathetic-adrenal axis by environmental enhancement or through genetic methods (by overexpressing BDNF in the hypothalamus), results in leanness, increased energy expenditure, and also upregulated hypothalamic VGF expression (Cao et al., 2011; Cao et al., 2010; Foglesong et al., 2016). Largely consistent with these studies, icv infusion of VGF peptide NERP-2 has been shown to result in increased energy expenditure and locomotor activity, and increased food intake, with the increases in locomotor activity and food intake found to be orexin-dependent (Toshinai et al., 2010).

In conclusion, the neurotrophin-inducible *Vgf* gene encodes a peptide precursor that is processed into several mature biologically active peptides (Lewis et al., 2015). TLQP-21 activates two receptors, the G protein-coupled complement 3a receptor (C3aR1) (Cero et al., 2014; Hannedouche et al., 2013) and the gC1q complement receptor (Chen et al., 2013), and recent data indicate that TLQP-21/C3aR1 is the predominant pathway by which peripheral actions of this peptide on lipolysis are transduced (Cero et al., 2016). Other VGF-derived peptides including TLQP-62, NERP-1, and NERP-2, are likely to act on distinct receptors that remain to be identified. Our studies further suggest that the lean, hypermetabolic phenotype of homozygous VGF knockout mice largely results from VGF ablation in embryonic neurons, and by comparison to the results of several studies discussed above, which have obtained overlapping results by administering various VGF-derived peptides to adult mice, suggest that VGF and/or its peptides play uniquely different roles in the developing and adult nervous system, particularly with respect to the circuits that control energy homeostasis. Future investigation into the metabolic function and signaling of these VGF-derived peptides may reveal novel pathways that can be manipulated in the adult nervous system and periphery to regulate energy balance.

Supplementary Material

Refer to Web version on PubMed Central for supplementary material.

Acknowledgments

Supported in part by: NIH grants DK071308 and MH086499 (SRS); DK074873, DK083568 and DK082724 (CB); Diabetes Action Research and Education Foundation (SRS); and an ADA Career Development Award (CB). CB is the recipient of a Hirschl-Weill-Caulier Career Scientist Award.

References

Bartolomucci A, La Corte G, Possenti R, Locatelli V, Rigamonti AE, Torsello A, Bresciani E, Bulgarelli I, Rizzi R, Pavone F, D'Amato FR, Severini C, Mignogna G, Giorgi A, Schinina ME, Elia G, Brancia C, Ferri GL, Conti R, Ciani B, Pascucci T, Dell'omo G, Muller EE, Levi A, Moles A. TLQP-21, a VGF-derived peptide, increases energy expenditure and prevents the early phase of diet-induced obesity. Proc Natl Acad Sci U S A. 2006; 103:14584–14589. [PubMed: 16983076]

Bartolomucci A, Possenti R, Mahata SK, Fischer-Colbrie R, Loh YP, Salton SR. The extended granin family: structure, function, and biomedical implications. Endocr Rev. 2011; 32:755–797. [PubMed: 21862681]

Briancon N, McNay DE, Maratos-Flier E, Flier JS. Combined neural inactivation of suppressor of cytokine signaling-3 and protein-tyrosine phosphatase-1B reveals additive, synergistic, and factor-

specific roles in the regulation of body energy balance. Diabetes. 2010; 59:3074–3084. [PubMed: 20876718]

Butler AA, Kozak LP. A recurring problem with the analysis of energy expenditure in genetic models expressing lean and obese phenotypes. Diabetes. 2010; 59:323–329. [PubMed: 20103710]

Cao L, Choi EY, Liu X, Martin A, Wang C, Xu X, During MJ. White to brown fat phenotypic switch induced by genetic and environmental activation of a hypothalamic-adipocyte axis. Cell Metab. 2011; 14:324–338. [PubMed: 21907139]

Cao L, Liu X, Lin EJ, Wang C, Choi EY, Riban V, Lin B, During MJ. Environmental and genetic activation of a brain-adipocyte BDNF/leptin axis causes cancer remission and inhibition. Cell. 2010; 142:52–64. [PubMed: 20603014]

Cero C, Razzoli M, Han R, Sahu B, Patricelli J, Guo ZK, Zaidman N, Miles J, O'Grady S, Bartolomucci A. The neuropeptide TLQP-21 opposes obesity via C3aR1-mediated enhancement of adrenergic-induced lipolysis. Mol Metab. 2016 in press.

Cero C, Vostrikov V, Verardi R, Severini C, Gopinath T, Braun PD, Sassano MF, Gurney A, Roth BL, Vulchanova L, Possenti R, Veglia G, Bartolomucci A. The TLQP-21 Peptide Activates the G-protein-coupled receptor C3aR1 via a Folding-upon-Binding Mechanism. Structure. 2014; 22:1744–1753. [PubMed: 25456411]

Chakraborty TR, Tkalych O, Nanno D, Garcia AL, Devi LA, Salton SR. Quantification of VGF- and pro-SAAS-derived peptides in endocrine tissues and the brain, and their regulation by diet and cold stress. Brain Res. 2006; 1089:21–32. [PubMed: 16631141]

Chen YC, Pristera A, Ayub M, Swanwick RS, Karu K, Hamada Y, Rice AS, Okuse K. Identification of a receptor for neuropeptide VGF and its role in neuropathic pain. J Biol Chem. 2013; 288:34638–34646. [PubMed: 24106277]

Christiansen CB, Svendsen B, Holst JJ. The VGF-Derived Neuropeptide TLQP-21 Shows No Impact on Hormone Secretion in the Isolated Perfused Rat Pancreas. Horm Metab Res. 2015

Cohen P, Zhao C, Cai X, Montez JM, Rohani SC, Feinstein P, Mombaerts P, Friedman JM. Selective deletion of leptin receptor in neurons leads to obesity. J Clin Invest. 2001; 108:1113–1121. [PubMed: 11602618]

Fargali S, Garcia AL, Sadahiro M, Jiang C, Janssen WG, Lin WJ, Cogliani V, Elste A, Mortillo S, Cero C, Veitenheimer B, Graiani G, Pasinetti GM, Mahata SK, Osborn JW, Huntley GW, Phillips GR, Benson DL, Bartolomucci A, Salton SR. The granin VGF promotes genesis of secretory vesicles, and regulates circulating catecholamine levels and blood pressure. FASEB J. 2014

Fargali S, Scherer T, Shin AC, Sadahiro M, Buettner C, Salton SR. Germline ablation of VGF increases lipolysis in white adipose tissue. J Endocrinol. 2012; 215:313–322. [PubMed: 22942234]

Foglesong GD, Huang W, Liu X, Slater AM, Siu J, Yildiz V, Salton SR, Cao L. Role of Hypothalamic VGF in Energy Balance and Metabolic Adaption to Environmental Enrichment in Mice. Endocrinology. 2016; 157:983–996. [PubMed: 26730934]

Galichet C, Lovell-Badge R, Rizzoti K. Nestin-Cre mice are affected by hypopituitarism, which is not due to significant activity of the transgene in the pituitary gland. PLoS One. 2010; 5:e11443. [PubMed: 20625432]

Hahm S, Fekete C, Mizuno TM, Windsor J, Yan H, Boozer CN, Lee C, Elmquist JK, Lechan RM, Mobbs CV, Salton SR. VGF is required for obesity induced by diet, gold thioglucose treatment and agouti, and is differentially regulated in POMC- and NPY-containing arcuate neurons in response to fasting. J. Neurosci. 2002; 22:6929–6938. [PubMed: 12177191]

Hahm S, Mizuno TM, Wu TJ, Wisor JP, Priest CA, Kozak CA, Boozer CN, Peng B, McEvoy RC, Good P, Kelley KA, Takahashi JS, Pintar JE, Roberts JL, Mobbs CV, Salton SR. Targeted deletion of the Vgf gene indicates that the encoded secretory peptide precursor plays a novel role in the regulation of energy balance. Neuron. 1999; 23:537–548. [PubMed: 10433265]

Hannedouche S, Beck V, Leighton-Davies J, Beibel M, Roma G, Oakeley EJ, Lannoy V, Bernard J, Hamon J, Barbieri S, Preuss I, Lasbennes MC, Sailer AW, Suply T, Seuwen K, Parker CN, Bassilana F. The identification of the C3a Receptor (C3AR1) as the target of the VGF derived peptide TLQP-21 in rodent cells. J Biol Chem. 2013; 288:27434–27443. [PubMed: 23940034]

Harno E, Cottrell EC, White A. Metabolic pitfalls of CNS Cre-based technology. Cell Metab. 2013; 18:21–28. [PubMed: 23823475]

Hasue F, Kuwaki T, Kisanuki YY, Yanagisawa M, Moriya H, Fukuda Y, Shimoyama M. Increased sensitivity to acute and persistent pain in neuron-specific endothelin-1 knockout mice. Neuroscience. 2005; 130:349–358. [PubMed: 15664691]

Jethwa PH, Warner A, Nilaweera KN, Brameld JM, Keyte JW, Carter WG, Bolton N, Bruggraber M, Morgan PJ, Barrett P, Ebling FJ. VGF-derived peptide, TLQP-21, regulates food intake and body weight in Siberian hamsters. Endocrinology. 2007; 148:4044–4055. [PubMed: 17463057]

Kim JW, Rhee M, Park JH, Yamaguchi H, Sasaki K, Minamino N, Nakazato M, Song DK, Yoon KH. Chronic effects of neuroendocrine regulatory peptide (NERP-1 and-2) on insulin secretion and gene expression in pancreatic beta-cells. Biochem Biophys Res Commun. 2015; 457:148–153. [PubMed: 25529453]

Levi A, Ferri GL, Watson E, Possenti R, Salton SR. Processing, distribution and function of VGF, a neuronal and endocrine peptide precursor. Cell Mol Neurobiol. 2004; 24:517–533. [PubMed: 15233376]

Lewis JE, Brameld JM, Jethwa PH. Neuroendocrine Role for VGF. Front Endocrinol (Lausanne). 2015; 6:3. [PubMed: 25699015]

Lin WJ, Jiang C, Sadahiro M, Bozdagi O, Vulchanova L, Alberini CM, Salton SR. VGF and its C-terminal peptide TLQP-62 regulate memory formation in hippocampus via a BDNF-dependent mechanism. J Neurosci. 2015; 35:10343–10356. [PubMed: 26180209]

May P, Rohlmann A, Bock HH, Zurhove K, Marth JD, Schomburg ED, Noebels JL, Beffert U, Sweatt JD, Weeber EJ, Herz J. Neuronal LRP1 functionally associates with postsynaptic proteins and is required for normal motor function in mice. Mol Cell Biol. 2004; 24:8872–8883. [PubMed: 15456862]

Melis MR, Sanna F, Succu S, Ferri GL, Argiolas A. Neuroendocrine regulatory peptide-1 and neuroendocrine regulatory peptide-2 influence differentially feeding and penile erection in male rats: sites of action in the brain. Regul Pept. 2012; 177:46–52. [PubMed: 22561139]

Mishiro-Sato E, Sasaki K, Matsuo T, Kageyama H, Yamaguchi H, Date Y, Matsubara M, Ishizu T, Yoshizawa-Kumagaye K, Satomi Y, Takao T, Shioda S, Nakazato M, Minamino N. Distribution of neuroendocrine regulatory peptide-1 and -2, and proteolytic processing of their precursor VGF protein in the rat. J Neurochem. 2010; 114:1097–1106. [PubMed: 20524965]

Moin AS, Yamaguchi H, Rhee M, Kim JW, Toshinai K, Waise TM, Naznin F, Matsuo T, Sasaki K, Minamino N, Yoon KH, Nakazato M. Neuroendocrine regulatory peptide-2 stimulates glucose-induced insulin secretion in vivo and in vitro. Biochem Biophys Res Commun. 2012; 428:512–517. [PubMed: 23111332]

Mori H, Hanada R, Hanada T, Aki D, Mashima R, Nishinakamura H, Torisu T, Chien KR, Yasukawa H, Yoshimura A. Socs3 deficiency in the brain elevates leptin sensitivity and confers resistance to diet-induced obesity. Nat Med. 2004; 10:739–743. [PubMed: 15208705]

Noble EE, Billington CJ, Kotz CM, Wang C. The lighter side of BDNF. Am J Physiol Regul Integr Comp Physiol. 2011; 300:R1053–R1069. [PubMed: 21346243]

Noli B, Brancia C, Pilleri R, D'Amato F, Messana I, Manconi B, Ebling FJ, Ferri GL, Cocco C. Photoperiod Regulates vgf-Derived Peptide Processing in Siberian Hamsters. PLoS One. 2015; 10:e0141193. [PubMed: 26555143]

Possenti R, Muccioli G, Petrocchi P, Cero C, Cabassi A, Vulchanova L, Riedl MS, Manieri M, Frontini A, Giordano A, Cinti S, Govoni P, Graiani G, Quaini F, Ghe C, Bresciani E, Bulgarelli I, Torsello A, Locatelli V, Sanghez V, Larsen BD, Petersen JS, Palanza P, Parmigiani S, Moles A, Levi A, Bartolomucci A. Characterization of a novel peripheral pro-lipolytic mechanism in mice: role of VGF-derived peptide TLQP-21. Biochem J. 2012; 441:511–522. [PubMed: 21880012]

Rempe D, Vangeison G, Hamilton J, Li Y, Jepson M, Federoff HJ. Synapsin I Cre transgene expression in male mice produces germline recombination in progeny. Genesis. 2006; 44:44–49. [PubMed: 16419044]

Ren H, Plum-Morschel L, Gutierrez-Juarez R, Lu TY, Kim-Muller JY, Heinrich G, Wardlaw SL, Silver R, Accili D. Blunted refeeding response and increased locomotor activity in mice lacking FoxO1 in synapsin-Cre-expressing neurons. Diabetes. 2013; 62:3373–3383. [PubMed: 23835335]

Sadahiro M, Erickson C, Lin WJ, Shin AC, Razzoli M, Jiang C, Fargali S, Gurney A, Kelley KA, Buettner C, Bartolomucci A, Salton SR. Role of VGF-derived carboxy-terminal peptides in energy

balance and reproduction: analysis of 'humanized' knockin mice expressing full length or truncated VGF. Endocrinology. 2015; 156:1724–1738. [PubMed: 25675362]

Saderi N, Buijs FN, Salgado-Delgado R, Merkenstein M, Basualdo MC, Ferri GL, Escobar C, Buijs RM. A role for VGF in the hypothalamic arcuate and paraventricular nuclei in the control of energy homeostasis. Neuroscience. 2014; 265:184–195. [PubMed: 24508747]

Salton SR, Ferri GL, Hahm S, Snyder SE, Wilson AJ, Possenti R, Levi A. VGF: a novel role for this neuronal and neuroendocrine polypeptide in the regulation of energy balance. Front Neuroendocrinol. 2000; 21:199–219. [PubMed: 10882540]

Silva JE. Physiological importance and control of non-shivering facultative thermogenesis. Front Biosci (Schol Ed). 2011; 3:352–371. [PubMed: 21196381]

Stephens SB, Schisler JC, Hohmeier HE, An J, Sun AY, Pitt GS, Newgard CB. A VGF-derived peptide attenuates development of type 2 diabetes via enhancement of islet beta-cell survival and function. Cell Metab. 2012; 16:33–43. [PubMed: 22768837]

Toshinai K, Yamaguchi H, Kageyama H, Matsuo T, Koshinaka K, Sasaki K, Shioda S, Minamino N, Nakazato M. Neuroendocrine regulatory peptide-2 regulates feeding behavior via the orexin system in the hypothalamus. Am J Physiol Endocrinol Metab. 2010; 299:E394–E401. [PubMed: 20551287]

Tsien JZ, Chen DF, Gerber D, Tom C, Mercer EH, Anderson DJ, Mayford M, Kandel ER, Tonegawa S. Subregion- and cell type-restricted gene knockout in mouse brain. Cell. 1996; 87:1317–1326. [PubMed: 8980237]

Virtue S, Even P, Vidal-Puig A. Below thermoneutrality, changes in activity do not drive changes in total daily energy expenditure between groups of mice. Cell Metab. 2012; 16:665–671. [PubMed: 23140644]

Watson E, Fargali S, Okamoto H, Sadahiro M, Gordon RE, Chakraborty T, Sleeman MW, Salton SR. Analysis of knockout mice suggests a role for VGF in the control of fat storage and energy expenditure. BMC Physiol. 2009; 9:19. [PubMed: 19863797]

Watson E, Hahm S, Mizuno TM, Windsor J, Montgomery C, Scherer PE, Mobbs CV, Salton SR. VGF ablation blocks the development of hyperinsulinemia and hyperglycemia in several mouse models of obesity. Endocrinology. 2005; 146:5151–5163. [PubMed: 16141392]

Yamaguchi H, Sasaki K, Satomi Y, Shimbara T, Kageyama H, Mondal MS, Toshinai K, Date Y, Gonzalez LJ, Shioda S, Takao T, Nakazato M, Minamino N. Peptidomic identification and biological validation of neuroendocrine regulatory peptide-1 and-2. J Biol Chem. 2007; 282:26354–26360. [PubMed: 17609209]

Zhu Y, Romero MI, Ghosh P, Ye Z, Charnay P, Rushing EJ, Marth JD, Parada LF. Ablation of NF1 function in neurons induces abnormal development of cerebral cortex and reactive gliosis in the brain. Genes Dev. 2001; 15:859–876. [PubMed: 11297510]

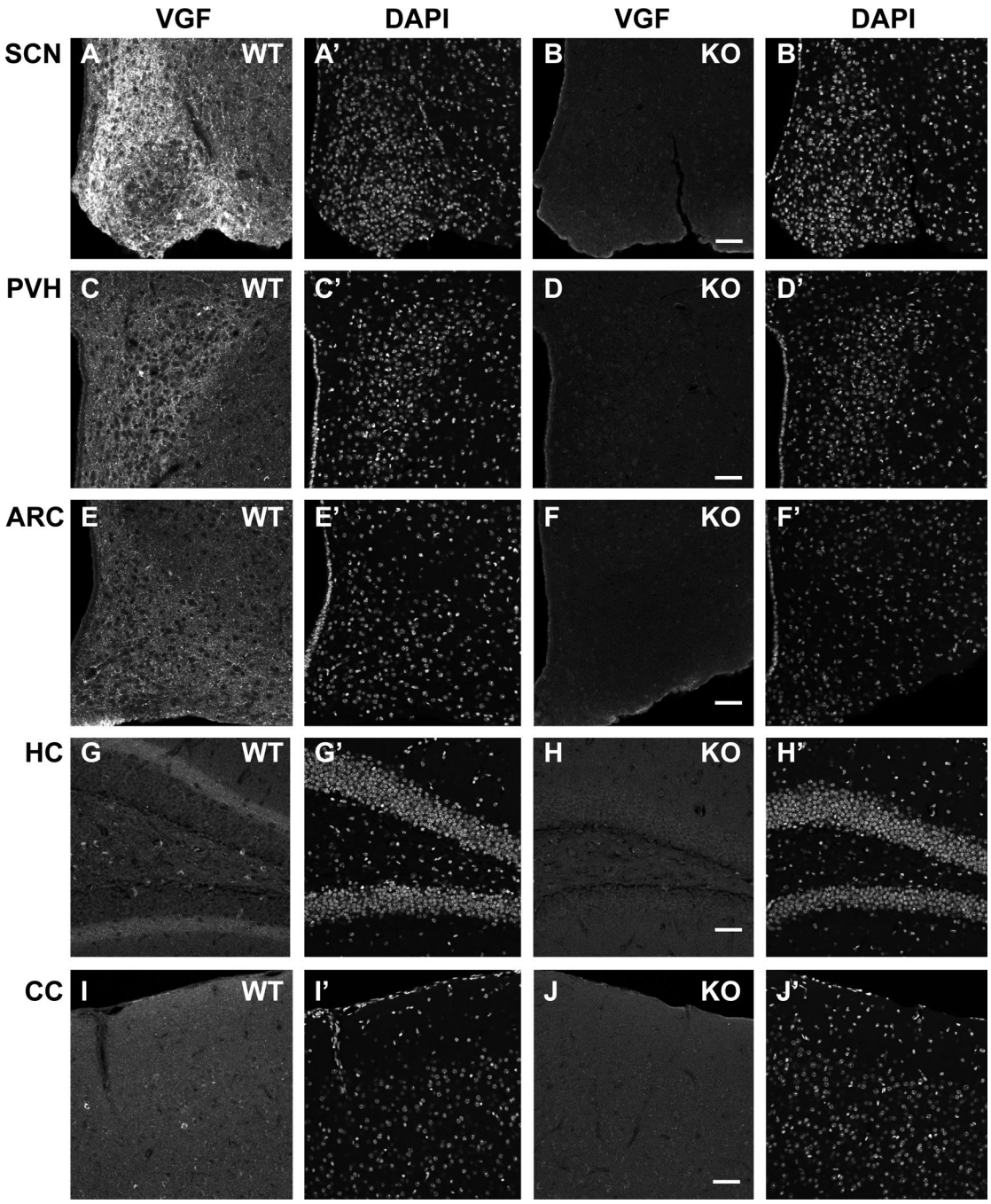

Figure 1. Immunohistochemical analysis of hypothalamic, hippocampal, and cortical VGF protein expression in male conditional knockout *Syn-Cre,Vgf*$^{flpflox/flpflox}$ mice

Adult male 4 month old *Syn-Cre,Vgf*$^{flpflox/flpflox}$ (panels B, D, F, H; scale bar 50 μm) and age- and sex-matched control *Syn-Cre,+/+* (panels A, C, E, G) mice were perfused, sectioned and immunohistochemically stained for VGF as described in 'Materials and Methods'. Staining with DAPI is shown in the adjacent photomicrographs (panels A'–H'). Brain regions stained by anti-VGF$_{588–617}$ (anti-AQEE-30) (Chakraborty et al., 2006) are as follows: hypothalamus, including suprachiasmatic nucleus (SCN) (panels A–B), paraventricular nucleus of the hypothalamus (PVH) (panels C–D), and arcuate nucleus

(ARC) (panels E–F); hippocampus (HC) (panels G–H); and cerebral cortex (CC) (somatosensory cortex layers 1 and 2/3) (panels I–J).

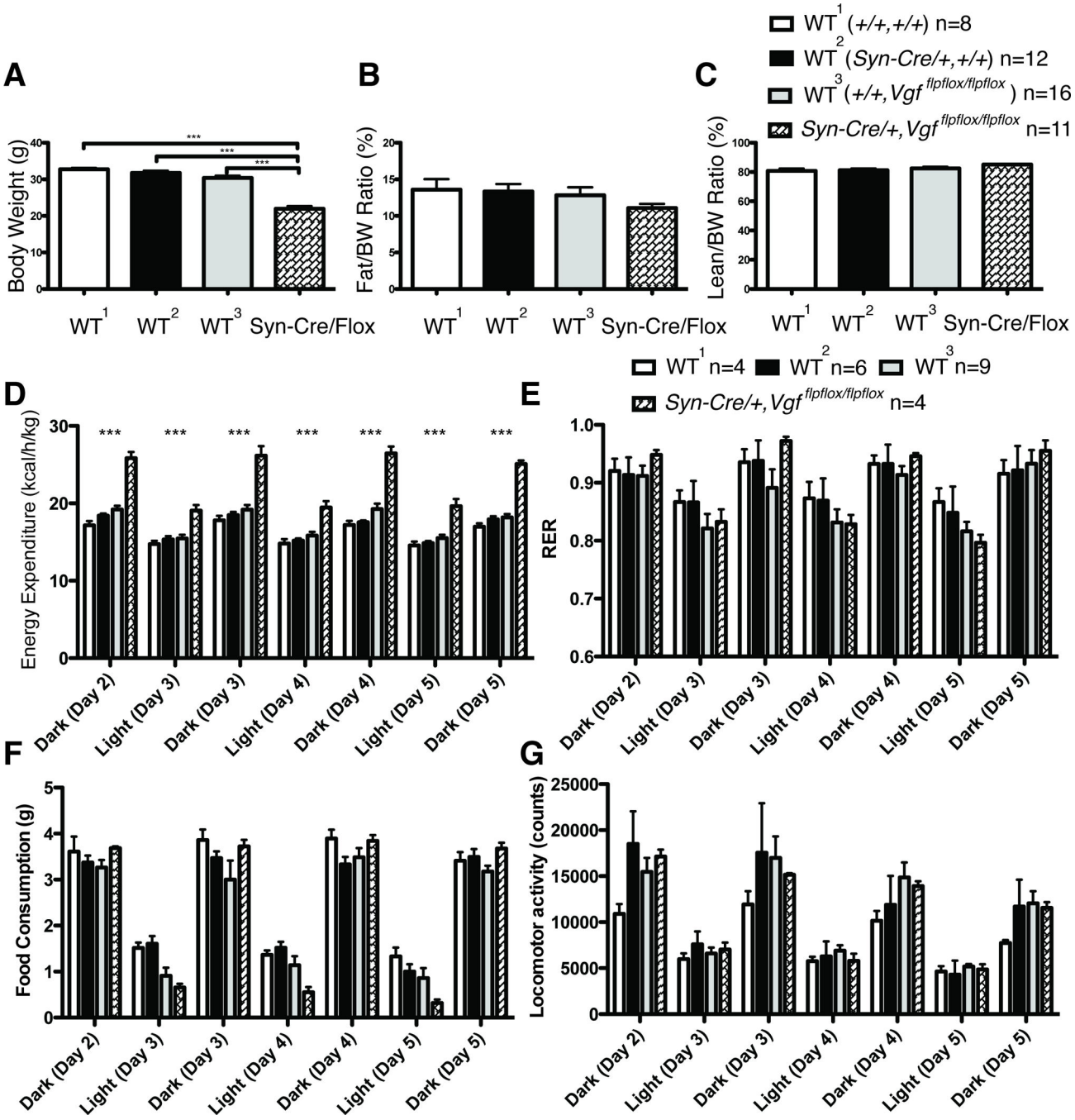

Figure 2. Metabolic analysis of adult male *Syn-Cre,Vgf*$^{flpflox/flpflox}$ mice fed a standard diet

Body weight (panel A), body composition including fat mass normalized to body weight (panel B) and lean mass normalized to body weight (panel C), energy expenditure (panel D), respiratory exchange ratio (RER) (panel E), food intake (panel F), and locomotor activity (panel G), were measured in *Syn-Cre,Vgf*$^{flpflox/flpflox}$ and wild type (*+/+,Vgf*$^{flpflox/flpflox}$), (+/+,+/+), or (*Syn-Cre,+/+*) male mice, fed a standard diet. Cohort sizes analyzed in panels A-C are shown above panel C, and in panels D-G, above panel E.

Panel A. Body weight data was analyzed by ANOVA with Bonferroni post hoc analysis, (3,43) = 57.64 ($P < 0.0001$; ***, $P < 0.001$ vs *Syn-Cre,* $Vgf^{flpflox/flpflox}$). Panels B and C. Body fat and lean mass normalized to body weight data were analyzed by ANOVA with Bonferroni post hoc analysis (n.s.). Panel D–G. Energy expenditure, RER, food intake, and locomotor activity data were analyzed by ANOVA with Bonferroni post hoc analysis between *+/+,* $Vgf^{flpflox/flpflox}$ and *Syn-Cre,* $Vgf^{flpflox/flpflox}$, respectively (***, $P<0.001$).

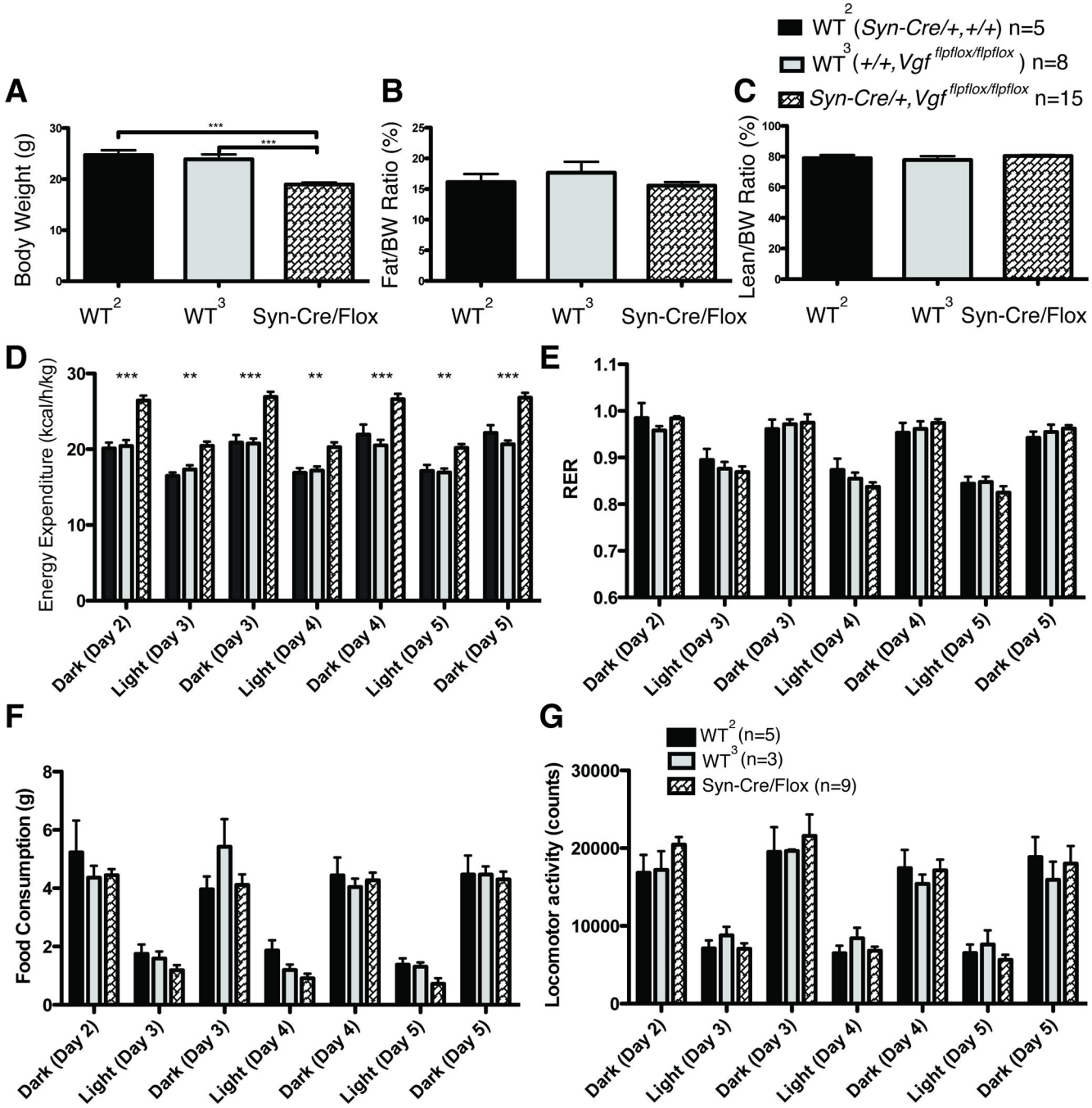

Figure 3. Metabolic analysis of adult female *Syn-Cre,Vgf*$^{flpflox/flpflox}$ mice fed a standard diet

Body weight (panel A), body composition including fat mass normalized to body weight (panel B) and lean mass normalized to body weight (panel C), energy expenditure (panel D), respiratory exchange ratio (RER) (panel E), food intake (panel F), and locomotor activity (panel G), were measured in *Syn-Cre,Vgf*$^{flpflox/flpflox}$ and wild type [(*+/+,Vgf*$^{flpflox/flpflox}$) or (*Syn-Cre,+/+*)] female mice, fed a standard diet. Cohort sizes analyzed in panels A–F are shown above panel C, and in panel G, above panel G.

Panel A. Body weight data was analyzed by ANOVA with Bonferroni post hoc analysis, $F(2,24) = 25.67$ ($P < 0.0001$; ***, $P < 0.001$ vs *Syn-Cre,* $Vgf^{flpflox/flpflox}$). Panels B and C. Body fat and lean mass normalized to body weight data were analyzed by ANOVA with Bonferroni post hoc analysis (n.s.). Panel D–G. Energy expenditure, RER, food intake and locomotor activity data were analyzed by ANOVA with Bonferroni's post hoc analysis between *+/+,* $Vgf^{flpflox/flpflox}$ and *Syn-Cre,* $Vgf^{flpflox/flpflox}$, respectively (**, $P<0.01$; ***, $P<0.001$).

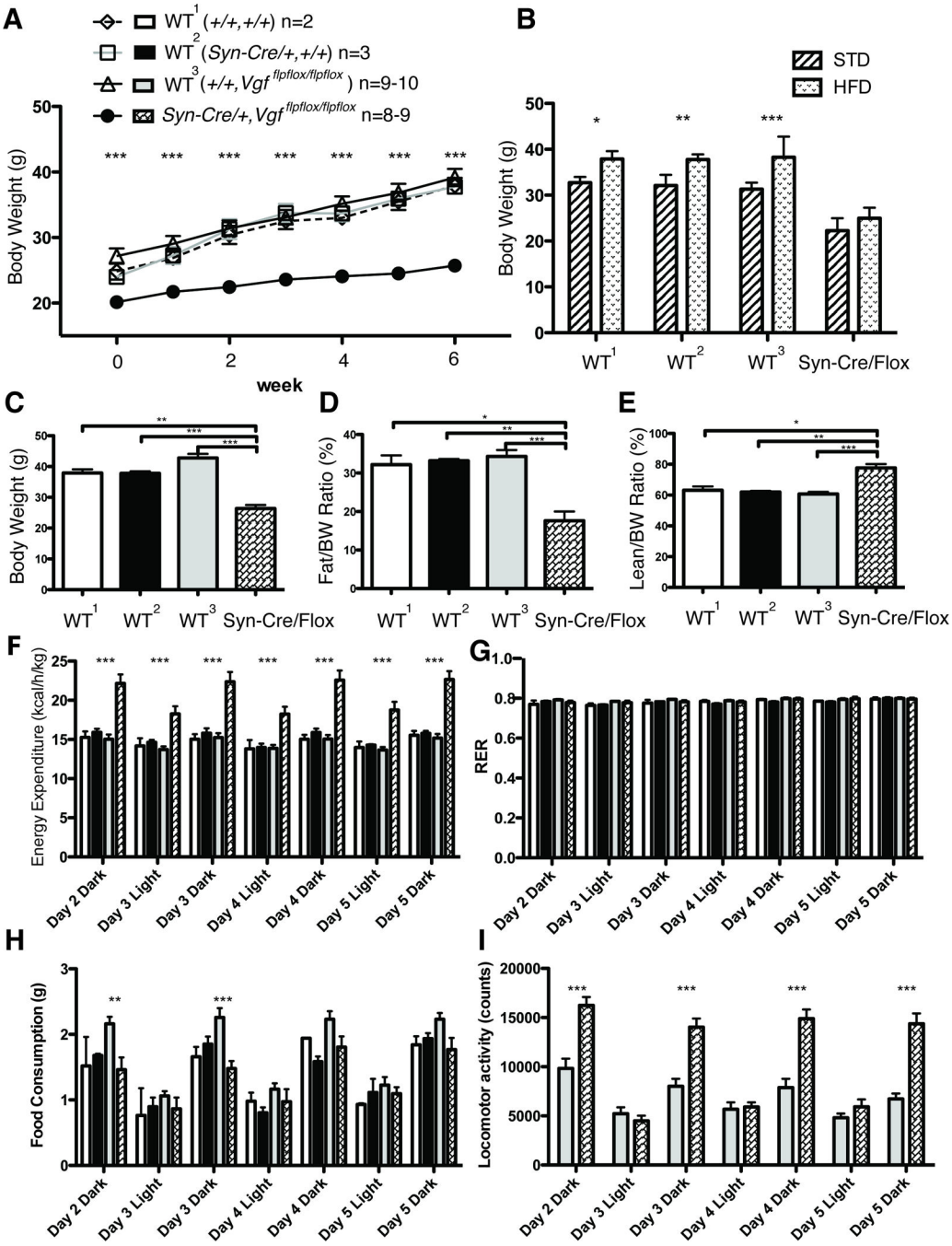

Figure 4. Metabolic analysis of adult male *Syn-Cre,Vgf*$^{flpflox/flpflox}$ mice fed a high-fat diet (HFD)

Body weight change over 6 weeks in mice fed a high fat diet (HFD) (panel A) was measured weekly, starting at 8–11 weeks of age, in *Syn-Cre,Vgf*$^{flpflox/flpflox}$ and wild type [(*+/+,Vgf*$^{flpflox/flpflox}$), (*Syn-Cre,+/+*), or (+/+,+/+)] male mice. In panel B, body weights of 12–14 week old wild type and *Syn-Cre,Vgf*$^{flpflox/flpflox}$ mice fed STD or HFD for 6 weeks are compared. After mice had completed 6 – 10 weeks on HFD, starting at 8–11 weeks of age, body weight (panel C), body composition including fat mass normalized to body weight (panel D) and lean mass normalized to body weight (panel E), energy expenditure (panel F),

respiratory exchange ratio (RER) (panel G), food intake (panel H), and locomotor activity (panel I), were measured in *Vgf*$^{flpflox/flpflox}$,*Syn-Cre* and wild type [(*Vgf*$^{flpflox/flpflox}$,*+/+*), (*Syn-Cre,+/+*), or (+/+,+/+)] male mice. Cohort sizes analyzed in panels A, and C–H are shown above panel A.

Panel A. Body weight change over 6 weeks on HFD was analyzed by ANOVA with Bonferroni post hoc analysis between *+/+, Vgf*$^{flpflox/flpflox}$ and *Syn-Cre,Vgf*$^{flpflox/flpflox}$ (***, P<0.001). Panel B. Body weights on STD or HFD were analyzed by ANOVA with Bonferroni post hoc analysis (*, P<0.05, **, P<0.01, ***, P<0.001). Cohort sizes: STD: (+/+, +/+ = 6; *Syn-Cre,Vgf*$^{+/+}$= 9; *+/+,Vgf*$^{flpflox/flpflox}$ = 13; *Syn-Cre,Vgf*$^{flpflox/flpflox}$ = 7), HFD: (+/+, +/+ = 2; *Syn-Cre,Vgf*$^{+/+}$= 3; *+/+,Vgf*$^{flpflox/flpflox}$ = 6; *Syn-Cre,Vgf*$^{flpflox/flpflox}$ = 6). Panel C. Body weight data was analyzed by ANOVA with Bonferroni post hoc analysis, $F(3,20) = 33.65$ ($P < 0.0001$; **, P<0.01; ***, $P < 0.001$ vs *Syn-Cre,Vgf*$^{flpflox/flpflox}$). Panel D. Body fat mass normalized to body weight was analyzed by ANOVA with Bonferroni post hoc analysis, $F(3,20) = 14.46$ ($P < 0.0001$; *, P<0.05; **, P<0.01; ***, $P < 0.001$ vs *Syn-Cre,Vgf*$^{flpflox/flpflox}$). Panel E. Body lean mass normalized to body weight was analyzed by ANOVA with Bonferroni post hoc analysis $F(3,20) = 16.06$ ($P < 0.0001$; *, P<0.05; **, P<0.01; ***, $P < 0.001$ vs *Syn-Cre,Vgf*$^{flpflox/flpflox}$). Panels F–H. Energy expenditure, RER and food intake data were analyzed by ANOVA with Bonferroni post hoc analysis between *+/+, Vgf*$^{flpflox/flpflox}$ and *Syn-Cre,Vgf*$^{flpflox/flpflox}$ respectively (**, P<0.01; ***, P<0.001). Panel I. Locomotor activity data was analyzed by ANOVA with Bonferroni post hoc analysis between *+/+, Vgf*$^{flpflox/flpflox}$ (n=9) and *Syn-Cre,Vgf*$^{flpflox/flpflox}$ (n=7) (***, P<0.001).

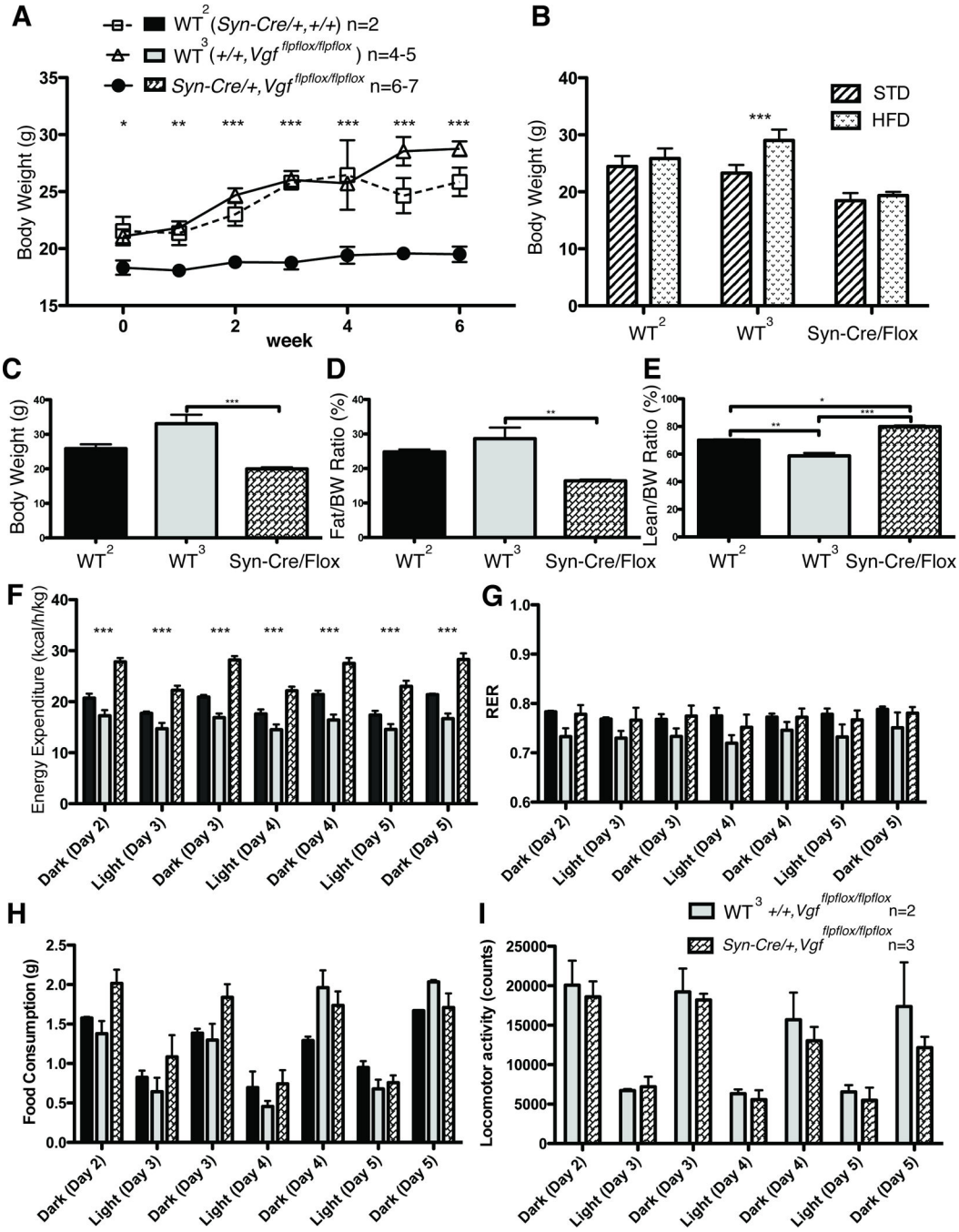

Figure 5. Metabolic analysis of adult female *Vgf*$^{flpflox/flpflox}$,*Syn-Cre* mice fed a high-fat diet (HFD)

Body weight change over 6 weeks on a high fat diet (HFD) (panel A) was measured weekly, starting at 8–11 weeks of age, in *Syn-Cre,Vgf*$^{flpflox/flpflox}$ and wild type [(*+/+,Vgf*$^{flpflox/flpflox}$) *or* (*Syn-Cre,+/+*)] female mice. In panel B, body weights of 9–14 week old wild type and *Syn-Cre,Vgf*$^{flpflox/flpflox}$ mice fed STD or HFD for 6 weeks are compared. After mice had completed 6 – 10 weeks on HFD, starting at 8–11 weeks of age, body weight (panel C), body composition including fat mass normalized to body weight (panel D) and lean mass normalized to body weight (panel E), energy expenditure (panel F), respiratory

exchange ratio (RER) (panel G), food intake (panel H), and locomotor activity (panel I), were measured in *Syn-Cre,Vgf*$^{flpflox/flpflox}$ and wild type [(*+/+,Vgf*$^{flpflox/flpflox}$) or (*Syn-Cre, +/+*)] female mice. Cohort sizes analyzed in panels A, and C-H, are shown above panel A. Panel A. Body weight change over 6 weeks on HFD was analyzed by ANOVA with Bonferroni post hoc analysis between *+/+, Vgf*$^{flpflox/flpflox}$ and *Syn-Cre,Vgf*$^{flpflox/flpflox}$ (*, P<0.05; **, P<0.01; ***, P<0.001). Panel B. Body weights on STD or HFD were analyzed by ANOVA with Bonferroni post hoc analysis (***, P<0.001). Cohort sizes: STD: (*Syn-Cre,Vgf*$^{+/+}$= 5; *+/+,Vgf*$^{flpflox/flpflox}$ = 5; *Syn-Cre,Vgf*$^{flpflox/flpflox}$ = 10), HFD: (*Syn-Cre,+/+*= 2; *+/+,Vgf*$^{flpflox/flpflox}$ = 3; *Syn-Cre,Vgf*$^{flpflox/flpflox}$ = 3). Panel C. Body weight data was analyzed by ANOVA with Bonferroni post hoc analysis, F (2,10) = 16.29 (P = 0.0007, ***, P < 0.001 vs *Syn-Cre,Vgf*$^{flpflox/flpflox}$). Panel D. Body fat mass normalized to body weight was analyzed by ANOVA with Bonferroni post hoc analysis, F (2,10) = 10.06 (P = 0.004; **, P<0.01 vs *Syn-Cre,Vgf*$^{flpflox/flpflox}$). Panel E. Body lean mass normalized to body weight data was analyzed by ANOVA with Bonferroni's post hoc analysis F (2,10) = 56.95 (P < 0.0001; *, P<0.05; **, P<0.01; ***, P < 0.001 vs *Syn-Cre,Vgf*$^{flpflox/flpflox}$). Panel F–H. Energy expenditure, RER and food intake data were analyzed by ANOVA with Bonferroni post hoc analysis between *+/+, Vgf*$^{flpflox/flpflox}$ and *Syn-Cre,Vgf*$^{flpflox/flpflox}$ respectively (***, P<0.001). Panel I. Locomotor activity data were analyzed by ANOVA with Bonferroni post hoc analysis between *+/+, Vgf*$^{flpflox/flpflox}$ (n=2) and *Syn-Cre,Vgf*$^{flpflox/flpflox}$ (n=3) (ns).